

# Metal-Bridging Mechanism for O–O Bond Cleavage in Cytochrome *c* Oxidase

Margareta R. A. Blomberg\* and Per E. M. Siegbahn

Department of Physics, Stockholm University, S-106 91 Stockholm, Sweden

Mårten Wikström

Helsinki Bioenergetics Group, Institute of Biotechnology, P.O. Box 65,  
00014 University of Helsinki, Helsinki, Finland

Received January 20, 2003

Density functional theory (B3LYP) has been applied to large models of the Fe(II)–Cu(I) binuclear center in cytochrome oxidase, investigating the mechanism of O–O bond cleavage in the mixed valence form of the enzyme. To comply with experimental information, the O<sub>2</sub> molecule is assumed to be bridging between iron and copper during the O–O bond cleavage, leading to the formation of a ferryl–oxo group and a cupric hydroxide. In accord with previous suggestions, the calculations show that it is energetically feasible to take the fourth electron needed in this reaction from the tyrosine residue that is cross-linked to one of the copper ligands, resulting in the formation of a neutral tyrosyl radical. However, the calculations indicate that simultaneous transfer of an electron and a proton from the tyrosine to dioxygen during bond cleavage leads to a barrier more than 10 kcal/mol higher than that experimentally determined. This may be overcome in two ways. If an extra proton in the binuclear center assists in the mechanism, the calculated reaction barrier agrees with experiment. Alternatively, the fourth electron might initially be supplied by a residue in the vicinity other than the tyrosine.

## I. Introduction

Cytochrome *c* oxidase is a member of the heme–copper oxidase family of enzymes that catalyze cell respiration in virtually all aerobic organisms. In these membrane-bound enzymes, O<sub>2</sub> binds to the ferrous–cuprous form of a binuclear heme–copper site (heme a<sub>3</sub> and Cu<sub>B</sub> in cytochrome *c* oxidases) in the largest protein subunit and is subsequently reduced to water. Electrons are donated to the site by a low spin heme in the vicinity. In the cytochrome *c* oxidases, the low spin heme receives electrons from cytochrome *c* via a bimetallic copper center (Cu<sub>A</sub>). Other heme–copper oxidases may use a hydroquinone as electron donor instead of cytochrome *c*.<sup>1</sup> Another key function of the heme–copper oxidases is that they also transform free energy from the exergonic reduction of O<sub>2</sub> to an electrochemical proton gradient for the synthesis of ATP, by translocation of protons across the membrane.<sup>2</sup>

O<sub>2</sub> binding to the iron of heme a<sub>3</sub> results in a state called compound A<sup>3</sup>. If the low spin heme (heme a) and the Cu<sub>A</sub> center are both oxidized (“mixed valence” form of the enzyme) so that no electron transfer can occur into the binuclear site, the next intermediate observed in the reaction is the so-called P<sub>M</sub> state of the binuclear site which is relatively stable in the absence of electron donors. Today, it has been established by several techniques that dioxygen is cleaved and effectively fully reduced already in this state.<sup>4–9</sup> Three of the four required electrons are donated by heme a<sub>3</sub> and by Cu<sub>B</sub>, resulting in a ferryl–cupric oxidation state of

\* To whom correspondence should be addressed. E-mail: mb@physto.se.

(1) Ferguson-Miller, S.; Babcock, G. T. *Chem. Rev.* **1996**, *96*, 2889–2907.

(2) Babcock, G. T.; Wikström, M. *Nature* **1992**, *356*, 301–309.

(3) Chance, B.; Saronio, C.; Leigh, J. S. *J. Biol. Chem.* **1975**, *250*, 9226–9237.

(4) Weng, L. C.; Baker, G. M. *Biochemistry* **1991**, *30*, 5727–5733.

(5) Watmough, N. J.; Cheesman, M. R.; Greenwood, C.; Thomson, A. J. *Biochem. J.* **1994**, *300*, 469–475.

(6) Wang, J.; Rumbley, J.; Ching, Y. C.; Takahashi, S.; Gennis, R. B.; Rousseau, D. L. *Biochemistry* **1995**, *34*, 9819–9825.

(7) Proshlyakov, D. A.; Ogura, T.; Shinzawa-Itoh, K.; Yoshikawa, S.; Kitagawa, T. *Biochemistry* **1996**, *35*, 8580–8586.

(8) Proshlyakov, D. A.; Pressler, M. A.; Babcock, G. T. *Proc. Natl. Acad. Sci. U.S.A.* **1998**, *95*, 8020–25.

(9) Fabian M.; Wong, W. W.; Gennis, R. B.; Palmer, G. *Proc. Natl. Acad. Sci. U.S.A.* **1999**, *96*, 13114–13117.

the site in  $P_M$ . Some evidence has been presented suggesting that the fourth electron may be donated by a tyrosine residue in the vicinity<sup>10</sup> that is covalently bonded to one of the three histidine ligands of  $Cu_B$ .<sup>11–13</sup> No intermediates are observed spectroscopically during conversion of compound A into the  $P_M$  state,<sup>1,8</sup> and therefore, the key events in cell respiration, i.e., activation of  $O_2$  and scission of the  $O-O$  bond, are still not fully understood. One way to nevertheless explore these important events is the application of quantum chemical calculations.<sup>14–17</sup>

Thus, in the present study large models of the binuclear center are used to investigate the mechanism for the  $O-O$  bond cleavage in the mixed valence form of cytochrome *c* oxidase. Previous studies with a similar goal used much smaller models.<sup>15,16</sup> On the basis of the results for the small models, a mechanism was suggested where in the first step a water molecule is cleaved on copper, and in the second step the  $O-O$  bond is cleaved with a low barrier, provided an extra proton is present at the binuclear center.<sup>16</sup> More recent calculations on the small models indicated that the extra proton actually must be involved in the reaction already when the water molecule is cleaved,<sup>17</sup> since otherwise unrealistically deep minima would be obtained. This new insight might change the conclusions about what is a possible mechanism for  $O-O$  bond cleavage. Furthermore, the previous calculations did not take into account the experimental indications concerning the origin of the copper bound oxygen in the product.<sup>18</sup> Therefore, new calculations have been performed, this time using much larger and more realistic models, focusing on mechanisms where the  $O_2$  molecule is bridging between the two metal atoms of the binuclear center during the  $O-O$  bond cleavage process. The mechanism suggested in the present study is different from the one previously suggested,<sup>16</sup> although there are some essential points of agreement. New light is shed on several mechanistic questions concerning the  $O-O$  bond activation.

## II. Computational Details

Modeling aspects and the methods used in the calculations on models for  $O_2$  reduction at the binuclear center in cytochrome oxidase are discussed in the following paragraphs.

The X-ray structure of the binuclear center in the mammalian enzyme is shown in Figure 1.<sup>11,19</sup> The binuclear center is composed

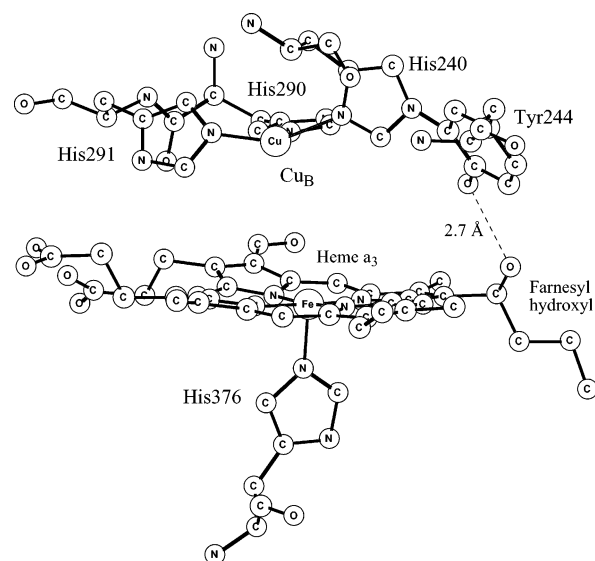


**Figure 1.** X-ray structure of the binuclear center.<sup>11</sup>

of two parts, a copper ( $Cu_B$ ) complex and an iron heme (heme  $a_3$ ) complex. Most of the calculations have been performed on models including both metal centers. In the main model of the  $Cu_B$  complex, the three histidine ligands are represented by imidazoles and the cross-linked His-Tyr residue is represented by a cross-linked imidazole–phenol unit. For the heme  $a_3$  complex, the model consists of a full but essentially unsubstituted porphyrin; only the farnesyl hydroxyl substituent is retained. A neutral imidazole replaces the axial histidine. In some calculations, smaller models are used, as described in the text. The X-ray structure is used as a starting point for the binuclear model.

For each structure considered, a full geometry optimization is first performed, using the hybrid density functional (DFT) B3LYP method.<sup>20</sup> In this first step, standard double- $\zeta$  basis sets are used for all light elements. For the metals (iron and copper), a nonrelativistic effective core potential (ECP) according to Hay and Wadt<sup>21</sup> is used. The valence basis set used in connection with this ECP is essentially of double- $\zeta$  quality. This basis set is labeled lacvp in the Jaguar program,<sup>22</sup> which is the main program used in these calculations. No restrictions are superimposed on the geometry optimizations, but it can be noted that qualitatively the X-ray structure of the binuclear center is maintained for all types of structures investigated. The energy is evaluated for the optimized geometries using the larger triple- $\zeta$  basis set, labeled lacv3p in Jaguar, extended with a single set of polarization functions on the heavy atoms. This final energy evaluation is also performed at the B3LYP level.

The inherent accuracy of the B3LYP functional has been estimated using the extended G3 benchmark set,<sup>23</sup> consisting of enthalpies of formation, ionization potentials, electron affinities, and proton affinities for first and second row molecules. This test has 376 entries, and the B3LYP functional obtains an average error

(10) Proshlyakov, D. A.; Pressler, M. A.; DeMaso, C.; Leykam, J. F.; DeWitt, D. L.; Babcock, G. T. *Science* **2000**, *290*, 1588–1591.

(11) Yoshikawa, S.; Shinzawa-Itoh, K.; Nakashima, R.; Yaono, R.; Yamashita, E.; Inoue, N.; Yao, M.; Fei, M. J.; Libeu, C. P.; Mizushima, T.; Yamaguchi, H.; Tomizaki, T.; Tsukihara, T. *Science* **1998**, *280*, 1723–1729.

(12) Ostermeier, C.; Harrenga, A.; Ermler, U.; Michel, H. *Proc. Natl. Acad. Sci. U.S.A.* **1997**, *94*, 10547–10553.

(13) Buse, G.; Soulimane, T.; Dewor, M.; Meyer, H. E.; Blüggel, M. *Protein Sci.* **1999**, *8*, 985–990.

(14) Moore, D. B.; Martinez, T. J. *J. Phys. Chem. A* **2000**, *104*, 2367–2374.

(15) Blomberg, M. R. A.; Siegbahn, P. E. M.; Babcock, G. T.; Wikström, M. *J. Inorg. Biochem.* **2000**, *80*, 261–269.

(16) Blomberg, M. R. A.; Siegbahn, P. E. M.; Babcock, G. T.; Wikström, M. *J. Am. Chem. Soc.* **2000**, *122*, 12848–12858.

(17) Blomberg, M. R. A.; Siegbahn, P. E. M. *J. Phys. Chem. B* **2001**, *105*, 9375–9386.

(18) Hansson, Ö.; Karlsson, B.; Aasa, R.; Vänngård, T.; Malmström, B. G. *EMBO J.* **1982**, *1*, 1295–1297.

(19) PDB structure 1OCC: Tsukihara, T.; Aoyama, H.; Yamashita, E.; Tomizaki, T.; Yamaguchi, H.; Shinzawa-Itoh, K.; Nakashima, R.; Yaono, R.; Yoshikawa, S. *Science* **1996**, *272*, 1136–44.

(20) Becke, A. D. *Phys. Rev.* **1988**, *A38*, 3098. Becke, A. D. *J. Chem. Phys.* **1993**, *98*, 1372. Becke, A. D. *J. Chem. Phys.* **1993**, *98*, 5648.

(21) Hay, P. J.; Wadt, W. R. *J. Chem. Phys.* **1985**, *82*, 299.

(22) JAGUAR 4.0; Schrödinger, Inc.: Portland, OR, 2000. See: Vacek, G.; Perry, J. K.; Langlois, J.-M. *Chem. Phys. Lett.* **1999**, *310*, 189–194.

(23) Curtiss, L. A.; Raghavachari, K.; Redfern, R. C.; Pople, J. A. *J. Chem. Phys.* **2000**, *112*, 7374–83.

of 4.27 kcal/mol.<sup>23</sup> A large part of the error comes from the set of 75 enthalpies of formation for large molecules. However, enthalpies of formation for large molecules, where a large number of new bonds are formed, should be the least relevant when studying reaction mechanisms where only a few bonds are formed or broken, and if this group is excluded, the B3LYP functional has an error of 3.29 kcal/mol (301 entries). For transition metals, there are no benchmarks due to the lack of accurate experimental numbers, but indications from normal metal–ligand bond strengths are that the errors are slightly larger, 3–5 kcal/mol.<sup>24</sup>

The activation energies are calculated as the energy difference between the reactant and a transition state structure. A full transition state optimization requires the calculation of the Hessian, i.e., second derivatives of the energy with respect to the nuclear coordinates. For the main model used in this study, containing about 100 atoms, explicit Hessian calculations are very time-consuming. Therefore, approximate transition states were determined by freezing one or two coordinates at different values, optimizing all the other degrees of freedom, and determining the maximum (or saddle point) on the potential energy surface thus obtained. The main frozen parameter is the O–O bond distance of the O<sub>2</sub> molecule to be split. For one case, the O–O bond cleavage transition state of the most likely mechanism, a Hessian was actually computed for a model containing 98 atoms, to confirm the character of the stationary point. Furthermore, as described in the text, in one case a much smaller model was used (containing about 50 atoms), and in this case an explicit Hessian calculation and a full transition state optimization was performed. For these calculations, the Gaussian program and the lanl2dz basis<sup>25</sup> were used. The calculated Hessians for the small model are also used to estimate zero-point, thermal, and entropy effects on the relative energies, applying the harmonic approximation. For this matter, Hessians are calculated also for the corresponding reactant structures.

The surrounding protein is treated as a dielectric medium. The approach used for calculating the effects of the dielectric medium is a Poisson–Boltzmann solver as implemented in the Jaguar program, with a probe radius of 1.40 Å corresponding to the water molecule. Water is a natural probe molecule, since it is the most physiological solvent, and in particular for the present enzyme there are water molecules present at the active site. Furthermore, it has been found that the results of the calculations are not very sensitive to the parameters of the solvent calculations. For example, the probe radius was changed to 2.50 Å for some of the optimized structures in the present study, and the relative energies were changed by less than one kcal/mol. The dielectric constant of the protein was chosen to be equal to 4 in line with previous suggestions for proteins. The dielectric effects on the relative energies due to the surrounding protein are in most cases found to be rather small, 0–2 kcal/mol, which is usually the case for reactions where the charge state of the cluster is constant. In a few cases, larger effects are obtained, which is then explicitly stated in the text.

(24) Siegbahn, P. E. M.; Blomberg, M. R. A. *Annu. Rev. Phys. Chem.* **1999**, *50*, 221–249.

(25) Frisch, M. J.; Trucks, G. W.; Schlegel, H. B.; Scuseria, G. E.; Robb, M. A.; Cheeseman, J. R.; Zakrzewski, V. G.; Montgomery, J. A., Jr.; Stratmann, R. E.; Burant, J. C.; Dapprich, S.; Millam, J. M.; Daniels, A. D.; Kudin, K. N.; Strain, M. C.; Farkas, O.; Tomasi, J.; Barone, V.; Cossi, M.; Cammi, R.; Mennucci, B.; Pomelli, C.; Adamo, C.; Clifford, S.; Ochterski, J.; Petersson, G. A.; Ayala, P. Y.; Cui, Q.; Morokuma, K.; Malick, D. K.; Rabuck, A. D.; Raghavachari, K.; Foresman, J. B.; Cioslowski, J.; Ortiz, J. V.; Stefanov, B. B.; Liu, G.; Liashenko, A.; Piskorz, P.; Komaromi, I.; Gomperts, R.; Martin, R. L.; Fox, D. J.; Keith, T.; Al-Laham, M. A.; Peng, C. Y.; Nanayakkara, A.; Gonzalez, C.; Challacombe, M.; Gill, P. M. W.; Johnson, B. G.; Chen, W.; Wong, M. W.; Andres, J. L.; Head-Gordon, M.; Replogle, E. S.; Pople, J. A. *Gaussian 98*; Gaussian, Inc.: Pittsburgh, PA, 1998.

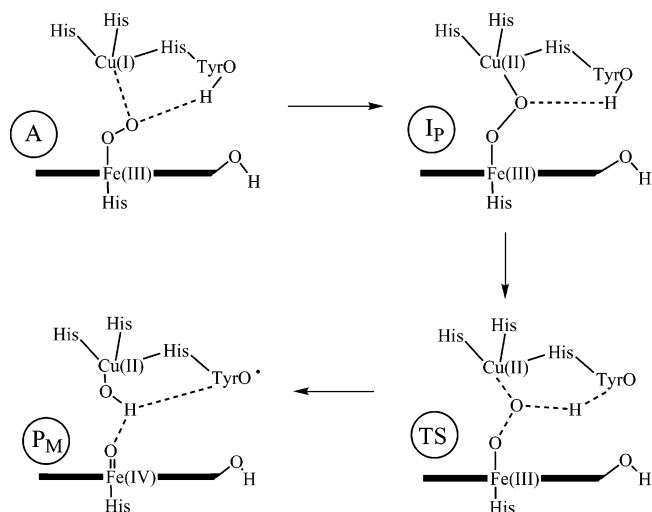


**Figure 2.** Originally suggested mechanism for O–O bond cleavage in the mixed valence enzyme.<sup>8</sup>

In studying mechanisms for biochemical reactions, one difficulty is describing the hydrogen bonding situation for different intermediate structures in a balanced way. In the enzyme, the hydrogen bonding is expected to be saturated during the whole reaction, while in the model systems only some of the hydrogen bonding opportunities are present. The changes in hydrogen bonding are usually much smaller when going from a reactant to the immediately following transition state. Therefore, in certain respects, it is simpler to determine activation energies than reaction energies. This means that the most reliable results of the present study are the calculated O–O bond activation energies relative to the preceding peroxide type of structure. The uncertainty in the calculated activation energies is estimated to be 3–5 kcal/mol, as already noted concerning the general accuracy in calculated relative energies using the B3LYP functional for transition metal containing systems. Furthermore, studies of many different metalloenzymes have shown that computed activation energies tend to be a few kilocalories per mole too high compared to what is obtained from experimental rate measurements.<sup>26</sup>

### III. Results and Discussion

The starting point for the present investigation of the O–O bond cleavage step is the mechanism suggested by Babcock and co-workers,<sup>8</sup> shown in Figure 2. This mechanism was built on results from resonance Raman spectroscopy on the mixed valence form of the enzyme, showing that the O–O bond is cleaved already at this level of reduction. Another reason for the suggestion of this mechanism is that the crystal structure<sup>11,12</sup> shows a covalent cross-link between one of the copper-ligated histidines, His240, and a tyrosine residue at the binuclear center, Tyr244, indicative of radical chemistry at the active site. One of the main features of the suggested mechanism is thus the formation of a tyrosyl radical at Tyr244. The mechanism also takes into account the results of isotope labeling experiments, indicating that the oxygen atom coordinated to Cu<sub>B</sub> in the product originates from molecular oxygen.<sup>18</sup> Previous calculations using small models indicated that the mechanism in Figure 2 would lead to too high a barrier.<sup>16</sup> A reinvestigation of this mechanism using

(26) Siegbahn, P. E. M. *Q. Rev. Biophys.* **2003**, *36*, 91–145.

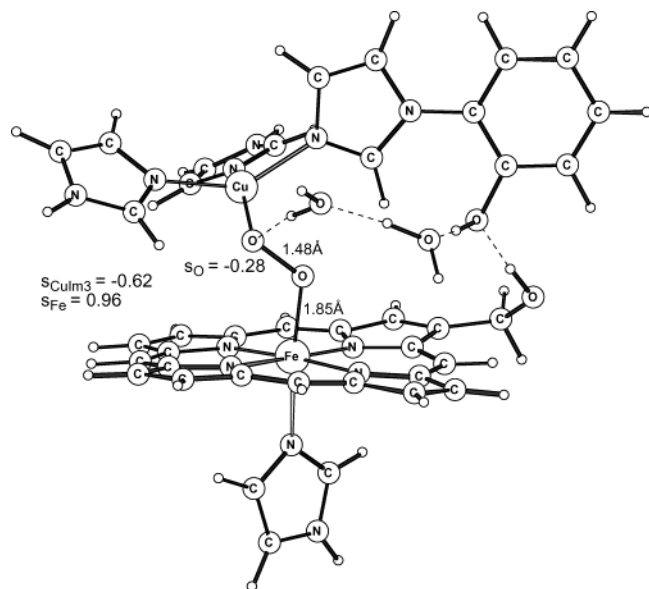


**Figure 3.** Optimized structure for a peroxide type of structure,  $I_p$ , including two water molecules.

large and more realistic models of the binuclear center is presented here together with a new, more feasible mechanism.

In subsection IIIa, the peroxide type of structure labeled  $I_p$  in Figure 2 is taken as a starting point, and the energy cost to cleave the O—O bond is calculated and compared to experimental data. In subsection IIIb, the further steps leading from the O—O cleavage transition state to the observed compound  $P_M$  with a tyrosyl radical are discussed, and in subsection IIIc, the first step, the formation of the unstable peroxide structure,  $I_p$ , from compound A is discussed. Subsection III d is devoted to comparisons to results from smaller models, and in the final subsection, III e, the presently suggested mechanism for the whole reaction from compound A to compound  $P_M$  is summarized and discussed. The main experimental fact, to which the present results will be compared, is that the lifetime of compound A is determined to be 200  $\mu$ s for the mixed valence enzyme, which corresponds to a free energy of activation of 12.4 kcal/mol using transition state theory. It is furthermore clear from experiment that no stable peroxide type of structure exists, indicating that any peroxide structure, like  $I_p$  in Figure 2, must be at least a few kcal/mol higher in energy than compound A. Finally, from experimental observations, it can be concluded that the A to  $P_M$  step should be slightly exergonic. It cannot be endergonic, since then  $P_M$  would not be observed, and it is not likely to be very exergonic either, considering the efficiency of the enzyme.

**IIIa. O—O Bond Activation ( $I_p$  to TS Step).** To investigate the activation energy for the mechanism in Figure 2, a model of the O—O metal-bridging structure  $I_p$  was constructed. In order to obtain a hydrogen bonding contact between the bridging  $O_2$  molecule and Tyr244, it was found that it is necessary to add two water molecules, see Figure 3. In the previous theoretical study using much smaller models of the binuclear center, it was shown that, due to steric hindrance within the copper complex, at least one water

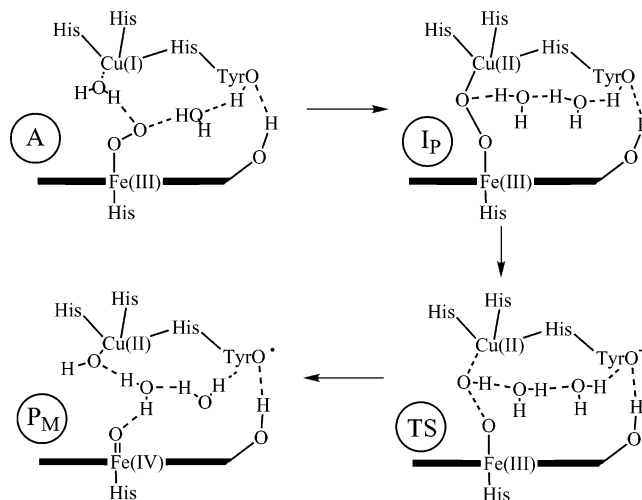


**Figure 4.** Originally suggested mechanism for O—O bond cleavage in the mixed valence enzyme slightly modified to include two water molecules.

molecule is needed to form a hydrogen bond between a copper coordinated oxygen atom and the tyrosine due to the cross-link.<sup>16</sup> Taking into account also the steric effects of the X-ray structure, showing that the hydroxyl group of Tyr244 is in hydrogen bonding contact to the farnesyl hydroxyl group of the heme  $a_3$  ring, and the direction of the open coordination site of  $Cu_B$  where  $O_2$  can coordinate, it is found that one more water molecule is needed in the link between  $O_2$  and Tyr244. It should be noted that the two water molecules are essential only for retaining the structure of the binuclear center, and in models which do not include the interaction between the farnesyl hydroxyl group and Tyr244, very similar results for the O—O bond cleavage activation energy are obtained using models with only one water molecule in the link between  $O_2$  and Tyr244, see further in following paragraphs.

Thus, the originally suggested mechanism, shown in Figure 2, has to be slightly modified to include two water molecules as shown in Figure 4. For the structure of compound A, before the bridging peroxide is formed, it is not obvious where the two water molecules should be placed. The structure given in Figure 4 was chosen since spectroscopic studies on compound A indicate that there is a water molecule in the vicinity of the copper atom.<sup>27</sup> The overall thermodynamics of the reaction in Figure 4 can be estimated from calculations on the separated copper and iron complexes for the following reaction:  $(His)_2Cu(I)(OH_2)(His-TyrOH) + (porph)Fe(III)O_2 \rightarrow (His)_2Cu(II)(OH)(His-TyrO^*) + (porph)Fe(IV)O-H_2O$ , thus omitting one water molecule which is not involved in the reaction, together with some hydrogen bonds and the electrostatic interaction between the two complexes, which thus are assumed to be constant during the reaction. At this level of approximation, the reaction is found to be exergonic by 5.6 kcal/mol. This result includes a rather large dielectric effect, making the reaction more exergonic by 7.8 kcal/mol. From these results, it is concluded that this type of reaction step is thermodynamically feasible.

(27) Ralle, M.; Verkhovskaya, M. L.; Morgan, J. E.; Verkhovsky, M. I.; Wikström, M.; Blackburn, N. J. *Biochemistry* **1999**, *38*, 7185–7194.

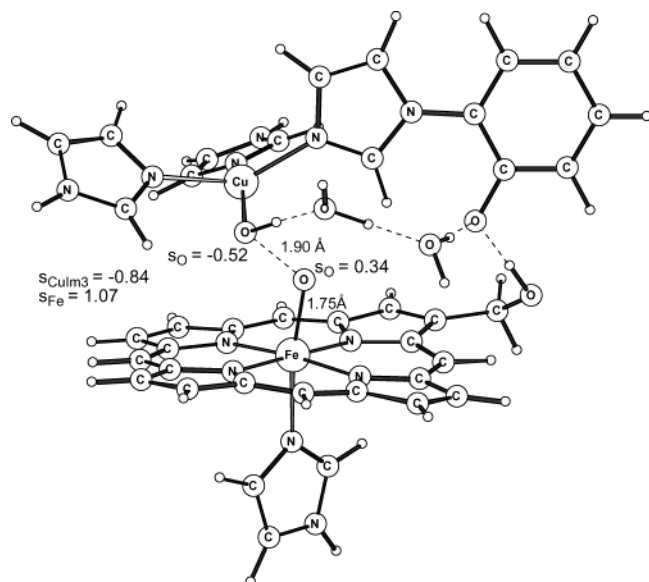


**Figure 5.** Approximate transition state for O–O bond cleavage according to the scheme in Figure 4.

In the next paragraph, the barrier for this reaction is estimated.

The energetics of O–O bond cleavage according to the scheme in Figure 4 are explored starting from the  $I_P$  peroxide structure in Figure 3. Different combinations of O–O bond elongation and proton motion along the hydrogen bonded chain from tyrosine toward the copper coordinated oxygen were tried. In agreement with the results of the previous theoretical study, using similar but much smaller models, it is found that the activation energy for cleaving the O–O bond according to this scheme is very high.<sup>16</sup> Since the model is large, a Hessian calculation is very costly, and only an approximate transition state was determined. The calculations indicate that the most advantageous reaction path for the O–O bond cleavage is obtained if a proton is first transferred from the tyrosyl hydroxyl group to the copper-ligated oxygen, forming an Fe–O–OH compound, with the OH-group coordinated to copper, and a tyrosinate. There is no minimum for this type of structure, and if the proton is not forced to stay at the peroxide, it therefore returns to the tyrosine. Forcing the proton to stay at the peroxide and successively increasing the O–O bond length yields a maximum at an O–O distance close to 1.9 Å, which is taken as an approximate transition state for the reaction scheme of Figure 4. The structure of the approximate transition state is given in Figure 5, together with the most important spin populations. The energy at this point is 20.6 kcal/mol above the bridging peroxide structure,  $I_P$ , in Figure 3. The activation energy relative to compound A should be higher than this value, see further in following paragraphs. To reach the  $P_M$  product from the structure where the O–O bond is cleaved, further rearrangements are needed, but since the activation energy for this mechanism is too high, these parts of the potential energy surface were not further investigated.

Thus, the mechanism in Figure 4 leads to a barrier that is too high, compared to the experimental lifetime of compound A, corresponding to a free energy of activation of only 12.4

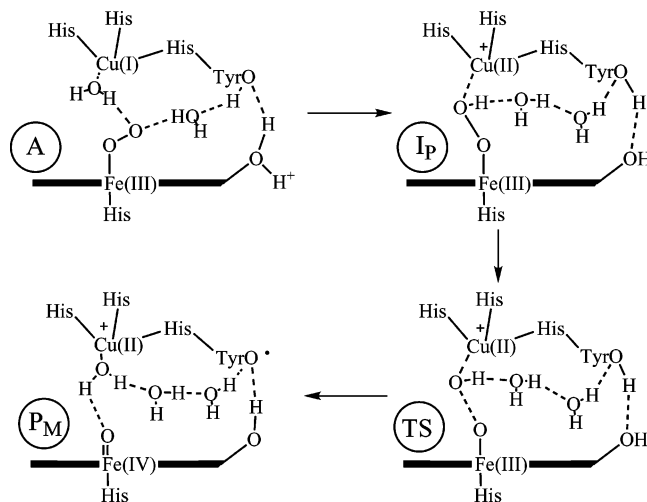


**Figure 6.** Protonated bridging mechanism with the extra proton at the farnesyl hydroxyl group. Other possibilities for the protonation are discussed in the text.

kcal/mol. Therefore, some modification of the mechanism has to be introduced. Previous calculations on small models indicate that the addition of either an extra electron or an extra proton has large effects on the potential energy surface, in both cases decreasing the O–O bond cleavage barrier.<sup>15,16</sup> Since the assumption generally made is that, in the mixed valence form of the enzyme, there is no other electron available, the number of electrons could not be changed. On the other hand, the number of protons present at the binuclear center for certain intermediates cannot so easily be determined experimentally, and one of the main difficulties in setting up a model for the quantum chemical calculations is to decide about the protonation state. Therefore, in the search for a feasible O–O bond cleavage mechanism, the scheme in Figure 4 was further modified to include one more proton, resulting in the mechanism of Figure 6. In the figure, it is assumed that compound A is protonated at the farnesyl hydroxyl group, as a result of a proton transfer via the K-channel in one of the reduction steps. Any other group that can be protonated in the vicinity of the binuclear center might as well be the source of this extra proton. In the first step, the proton is transferred to dioxygen via the hydrogen bonded chain of water molecules, and at the same time, an electron transfer from copper to the iron complex occurs, yielding the peroxide type of structure labeled  $I_P$  in Figure 6. A rearrangement of the water molecules is also necessary to allow the formation of the dioxygen bridge between the metal ions. The energy required to transfer the proton to the active site cannot be calculated using the present model, but since no peroxide structure is observed experimentally it is clear that this step has to be endergonic by a few kilocalories per mole. The reaction energy for the scheme in Figure 6, starting from the metal-bridging protonated peroxide structure  $I_P$ , can be estimated from the following reaction:  $(\text{His})_2\text{Cu}(\text{II})(\text{His-TyrOH}) + (\text{porph})\text{Fe}(\text{III})\text{O}_2\text{H} \rightarrow (\text{His})_2\text{Cu}(\text{II})(\text{His-TyrO}^*) + (\text{porph})\text{Fe}(\text{IV})\text{O}-\text{H}_2\text{O}$ , thus omitting both water molecules which are not involved in the chemical transformation. Calculations on the separated copper and iron complexes for this reaction, thus omitting also some hydro-

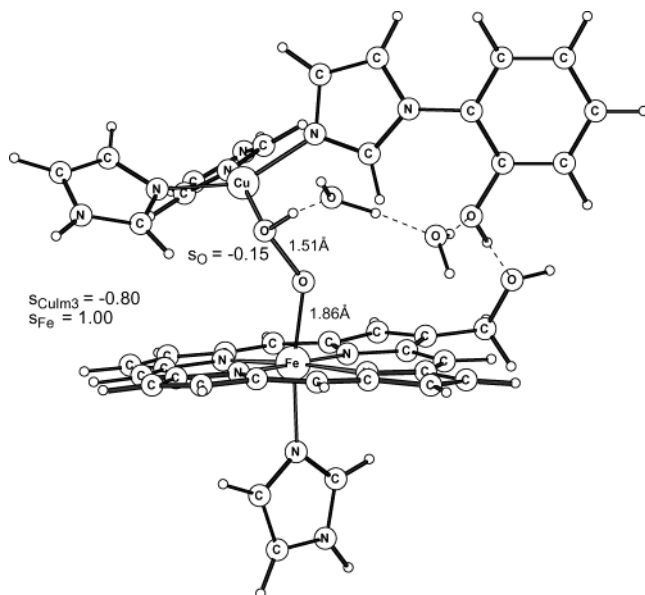


**Figure 7.** Optimized structure for a peroxide structure  $I_P$  including an extra proton.

gen bonds and the electrostatic interaction between the two complexes, which in this model thus are assumed to be constant during the reaction, give an exergonic reaction by 8.6 kcal/mol, which includes a rather large dielectric effect of 4.3 kcal/mol making the reaction more exergonic. Including the first proton transfer step, the mechanism in Figure 6 is thus estimated to be exergonic by a few kilocalories per mole less than 8.6 kcal/mol and is thus thermodynamically feasible.

The optimized structure of the peroxide compound  $I_P$  of Figure 6 is shown in Figure 7, and starting from this structure, the O—O bond length is successively increased, yielding a maximum at a value of about 2.0 Å. This maximum is taken as the transition state for the O—O bond cleavage, and the structure is shown in Figure 8 together with the most important spin populations. In this point, a Hessian was actually calculated, giving one imaginary frequency of 281  $\text{cm}^{-1}$ , corresponding to the O—O bond stretch, and a low gradient, showing that the structure corresponds well to the O—O bond cleavage transition state. The energy at this point is calculated to be 11.4 kcal/mol higher than the peroxide reactant  $I_P$  of Figure 7, and the activation energy relative to compound A is thus estimated to be a few kilocalories per mole higher in energy. This mechanism therefore seems to be in reasonable agreement with the experimental value for the free energy of activation of 12.4 kcal/mol.

The computed potential energy surfaces for stretching the O—O bond are sketched in Figure 9 for the two mechanisms shown in Figures 4 and 6, respectively, each one starting from its own unstable peroxide type of structure labeled  $I_P$  in the figures. From Figure 9, it can be seen that the energy changes for stretching the O—O bond behave rather similarly for the two mechanisms, but with a dramatic effect of about 9 kcal/mol decrease of the barrier with the addition of a proton to the binuclear center. The main conclusion of the present investigation is that, in the mixed valence situation with no other electron available at the binuclear center,

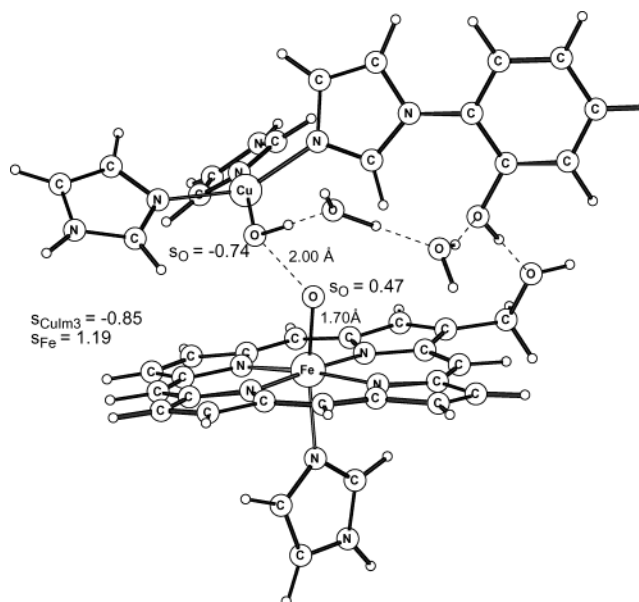


**Figure 8.** Transition state for O—O bond cleavage obtained for the model including an extra proton. The computed imaginary frequency is 281  $\text{cm}^{-1}$ .

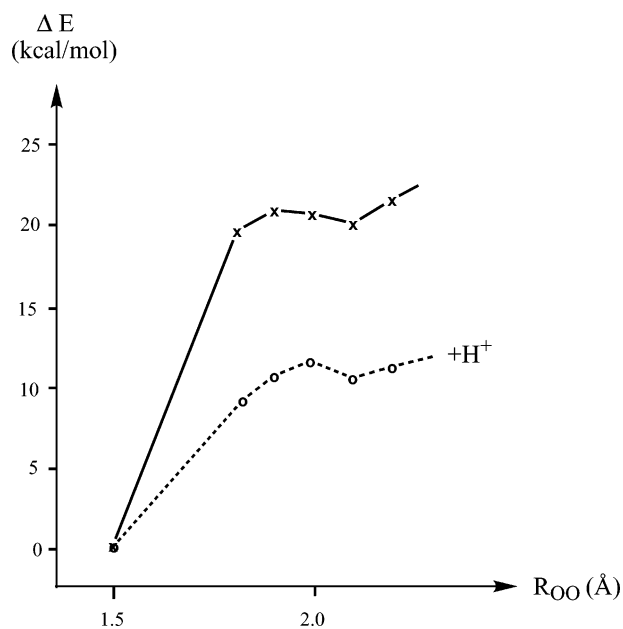


**Figure 9.** Calculated energy changes upon stretching the O—O bond, relative to the peroxide structure  $I_P$  for the mechanism in Figure 4 (—) and for the mechanism in Figure 6 with an extra proton (---).

molecular oxygen has to be protonated before the cleavage of the O—O bond, and that the proton cannot be provided by the tyrosine residue leaving a tyrosinate behind.

**IIIb. Completing the O—O Bond Cleavage (TS to  $P_M$  Step).** In Figure 9, both potential energy surfaces for the O—O bond cleavage have a shallow minimum immediately after the maximum is reached, with an O—O bond distance of about 2.1 Å. For the protonated mechanism, which is the only one discussed in this section, the energy of the minimum is about 1 kcal/mol lower than at the transition state, and upon further increase of the O—O bond distance, the energy increases slowly. The electronic structure at this minimum is very similar to the one in the transition state in Figure 8, with the only minor difference being that another 0.1  $\beta$

electrons are shifted from iron to the copper-ligated oxygen atom. The reaction so far, starting from the Fe(III)–peroxide structure,  $I_P$ , can be described as a transfer of one electron ( $\beta$ ) from iron (or an Fe–O antibonding  $\pi^*$ -orbital) into the antibonding  $\sigma^*$ -orbital of the O–O bond. This leaves effectively a one-electron bond between the two oxygens, which explains the existence of the minimum. A similar minimum is found for the O–O bond cleavage process in a biomimetic iron complex,<sup>28</sup> and also in an excited state of hydrogen peroxide. It is further interesting to note that the Fe–O bond length at the minimum is 1.67 Å, showing that the Fe(IV)=O double bond is almost completely formed at this point. To complete the heterolytic cleavage of the O–O bond, another electron ( $\alpha$ ) needs to be transferred into the O–O antibonding  $\sigma^*$ -orbital. Ideally, to reach the  $P_M$  product of the scheme in Figure 6, this electron should be taken from tyrosine. However, upon further increase of the O–O bond by a few tenths of an ångström, the energy goes up without any further electron transfer, only a slight shift of the spin from the iron–oxo oxygen to the copper ligated oxygen. One reason for this reluctance of the tyrosyl electron to move could be that tyrosyl radicals need to be deprotonated to become stable enough, as seen for example for photosystem II<sup>29</sup> and ribonucleotide reductase.<sup>30</sup> The hydrogen bonding in the structure in Figure 8 prevents the proton of the tyrosyl hydroxyl group to move to the copper-ligated hydroxyl group, forming a water ligand on copper as indicated in the  $P_M$  structure in Figure 6. Therefore, the hydrogen bonding chain was shifted such that the tyrosyl hydroxyl proton donates a hydrogen bond to the water molecule, and at the end, the second water molecule donates a hydrogen bond to the copper-ligated hydroxyl group, see Figure 10. This rearrangement was done for an O–O distance of 2.2 Å, and the new structure was optimized with the O–O distance frozen, giving an energy of 11.5 kcal/mol. This value is almost identical to the value of 11.3 kcal/mol obtained for an O–O distance of 2.2 Å with the original hydrogen bonding pattern. However, the electronic structure is different; with the new hydrogen bonding pattern, a second electron has been transferred into the O–O antibonding orbital, and the heterolytic O–O bond cleavage can be completed. When the freezing is released and the structure is fully optimized, the O–O bond distance increases and the energy decreases to 5.4 kcal/mol below the  $I_P$  peroxide structure, see Figure 10. The optimized structure is shown in Figure 11 together with the most important spin populations. From this figure, it can be seen that the second electron in the O–O bond cleavage is actually taken from the porphyrin ring, not from the tyrosine as expected. It is clear from experimental results that this cannot be the electronic structure of  $P_M$ , and therefore, there must be another step involved, transferring an electron from tyrosine to the porphyrin and a proton from

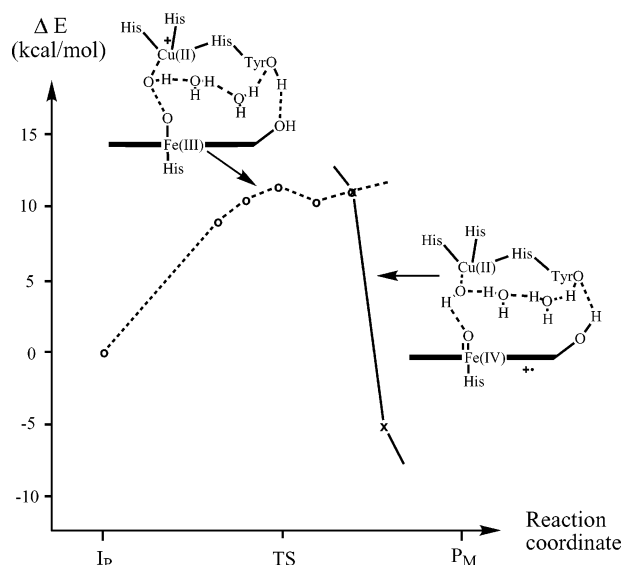


**Figure 10.** Calculated potential energy surface for the O–O activation starting at the peroxide type of structure  $I_P$  for the model including an extra proton.

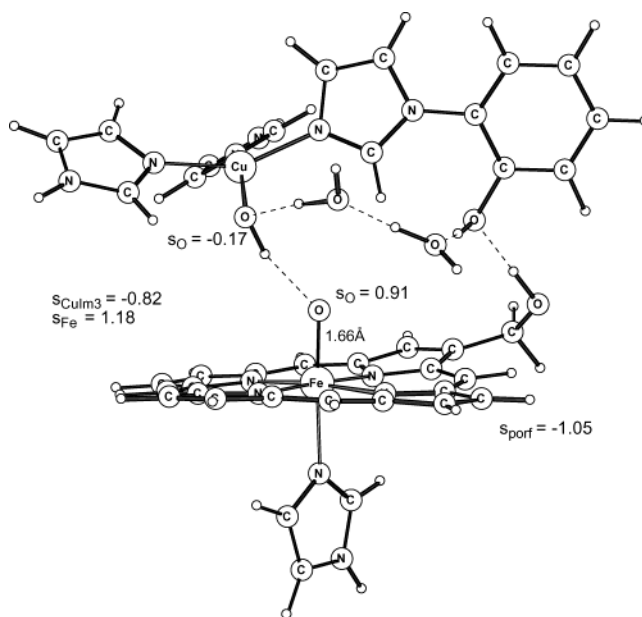


**Figure 11.** Optimized structure for the initial product of the O–O bond cleavage in the model including an extra proton.

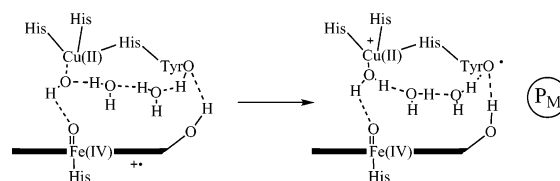


**Figure 12.** Last step in the O–O bond cleavage reaction for the protonated mechanism.

tyrosine to the copper-ligated hydroxyl group, as depicted in the scheme in Figure 12. The energetics of such a step have been investigated, and the product with a tyrosyl radical (see Figure 13) is found to be lower in energy than the porphyrin radical, which explains the fact that the porphyrin radical is never observed. It should be noted that the energetics of this part of the reaction are very difficult to describe accurately, since there are many different possible

(28) Bassan, A.; Blomberg, M. R. A.; Siegbahn, P. E. M.; Que, L., Jr. *J. Am. Chem. Soc.* **2002**, *124*, 11056–11063.

(29) Barry, B. A.; Babcock, G. T. *Proc. Natl. Acad. Sci. U.S.A.* **1987**, *84*, 7099.

(30) Ehrenberg, A.; Reichard, P. *J. Biol. Chem.* **1972**, *247*, 3485–3588.

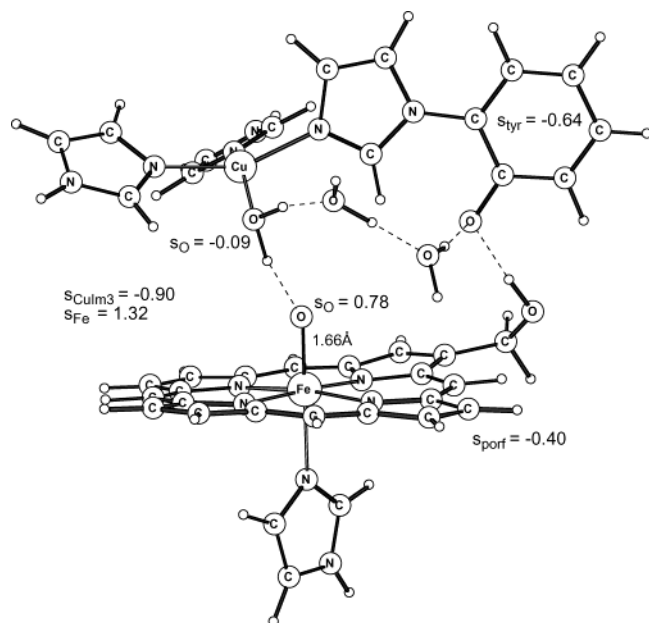


**Figure 13.** Optimized structure for the final product of the O–O bond cleavage in the model including an extra proton.

hydrogen bonding patterns, and the energy seems to be quite sensitive to these patterns. It is therefore possible that the formation of a porphyrin radical could be an artifact of the present model and never occurs in the enzyme.

To summarize this section, the heterolytic cleavage of the O–O bond starting from the peroxide type of structure occurs in two steps, corresponding to the first two steps in the orbital diagram in Figure 14. The first step involves an electron transfer ( $\beta$  electron) from Fe or an Fe–O antibonding orbital into the O–O antibonding orbital. This process gives rise to a transition state and a weak minimum with some remaining O–O bonding. This  $\beta$  electron transfer increases the number of unpaired  $\alpha$  electrons on Fe and O1, and it increases the number of unpaired  $\beta$  electrons on O2, as can be seen by comparing the population analysis for the first and second structure in Figure 14. In the second step, the second electron ( $\alpha$  electron) is transferred into the O–O antibonding orbital

from some other part of the binuclear center, and the heterolytic O–O bond cleavage is completed. This second step occurs as a curve crossing, as shown in Figure 10. This  $\alpha$  electron transfer increases the number of unpaired  $\alpha$  electrons on O1, and it decreases the number of unpaired  $\beta$  electrons on O2, as can be seen by comparing the population analysis for the second and third structure in Figure 14. The calculations further indicate that the source of the second electron initially is the porphyrin, giving rise to an unpaired  $\beta$  electron on the porphyrin, as can be seen in the third structure in Figure 14. In this case, a third step would be involved, since experiment has established that compound P<sub>M</sub> does not have a porphyrin radical. In the orbital diagram in Figure 14, the third step is indicated to involve an electron transfer ( $\alpha$  electron) from tyrosine to the porphyrin, resulting in the suggested tyrosyl radical in P<sub>M</sub>.

**IIIc. Compound A Activation (A to I<sub>P</sub> Step).** So far, the O–O bond activation has been discussed with respect to a peroxide type of structure, labeled I<sub>P</sub>. Since the peroxide structure is not observed experimentally, the activation energy should be referred to the observed compound A, having an O<sub>2</sub> molecule weakly bound to the iron center of heme a<sub>3</sub>. In a first attempt to describe compound A, calculations were performed on a model according to the scheme in Figure 4, i.e., without the extra proton. The optimized structure is shown in Figure 15, and the calculated energy relative to the peroxide type of structure, I<sub>P</sub>, in Figure 3 is +5.7 kcal/mol, which includes a dielectric effect of 2.6 kcal/mol raising the energy of compound A. In calculations on smaller models, which will be described in following paragraphs, it was found that there is an entropy effect of about 7 kcal/mol, raising the peroxide structure relative to the dioxygen structure. If such an entropy effect is included, the calculations thus give a free energy for compound A that is only slightly lower than that for the peroxide compound I<sub>P</sub>. Since the peroxide structure is not observed experimentally, it is clear that the peroxide structure I<sub>P</sub> must be at least a few kilocalories per mole higher in energy than compound A. At this point, it should be remembered that the intrinsic

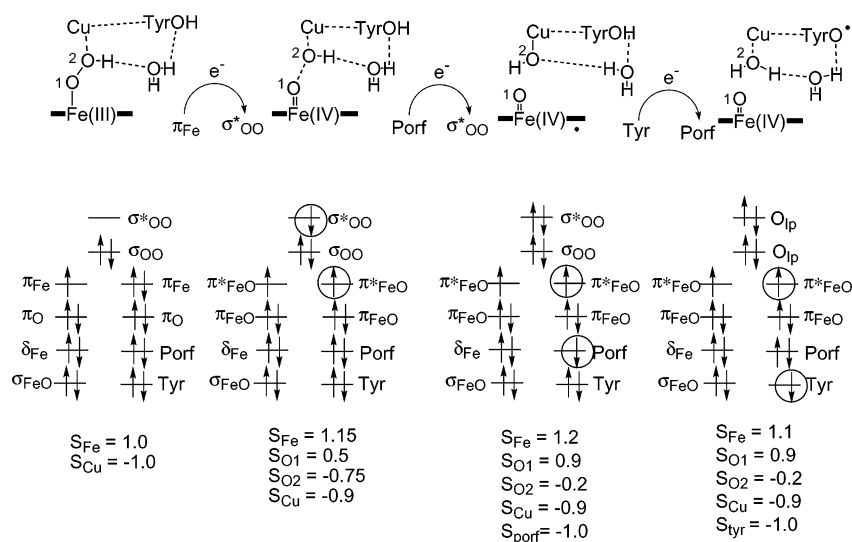


**Figure 14.** Orbital analysis of the O–O bond cleavage reaction.

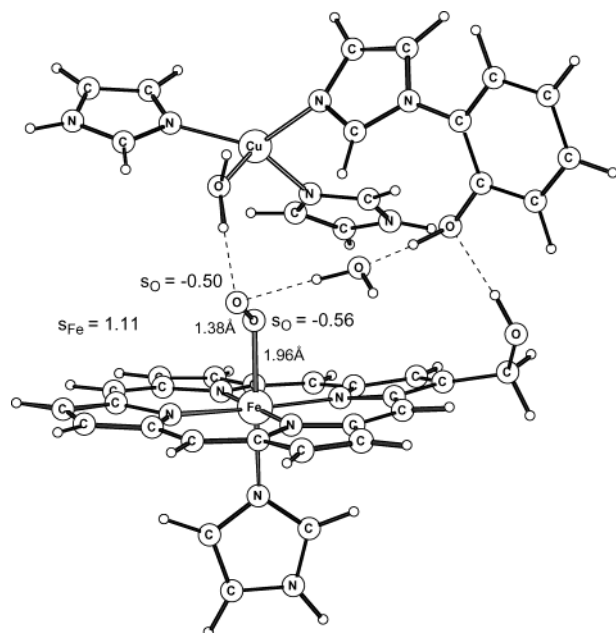


**Figure 15.** Optimized structure for compound A using the model including two water molecules.

uncertainty in the computed relative energies is 3–5 kcal/mol, as discussed in section II, and that the extra uncertainty in the relative energy of structures having quite different hydrogen bonding patterns should be added. Therefore, to obtain the O–O bond cleavage barrier relative to compound A, it is assumed that the peroxide structure  $I_P$  is 5 kcal/mol above the dioxygen structure, giving an occupancy of less than 0.1% of the peroxide structure, assuming thermodynamic equilibrium. Adding this value to the computed barrier of 20.6 kcal/mol relative to the peroxide structure  $I_P$  for the nonprotonated mechanism gives an estimated total barrier for the mechanism in Figure 4 of 25.6 kcal/mol. The experimental value is 12.4 kcal/mol, and the mechanism in Figure 4 clearly must be ruled out.

It was concluded that an extra proton is needed at the binculear center to make it possible to cleave the O–O bond with a low enough barrier in the mixed valence form of the enzyme. It is, however, not possible within the present model to calculate the energetics of the proton transfer occurring between compound A and compound  $I_P$  of the scheme in Figure 6. But since no peroxide structure is observed experimentally, it is clear that this step has to be endergonic. Thus, on a similar basis as for the unprotonated mechanism in Figure 4, it is assumed that the compound A to peroxide  $I_P$  step is 5 kcal/mol endergonic. Adding this energy to the computed barrier of 11.4 kcal/mol starting at the  $I_P$  structure gives a total barrier of 16.4 kcal/mol for the protonated mechanism of Figure 6, in good agreement with the experimental value of 12.4 kcal/mol.

**III.d. Results from Smaller Models.** To complete the picture given by the model calculations, some results for the metal bridging protonated mechanism for O–O bond cleavage already discussed, but using smaller models, will be described in this section. The calculations were done starting from the smallest model and increasing the size of the model as the computer resources increased. However, the results

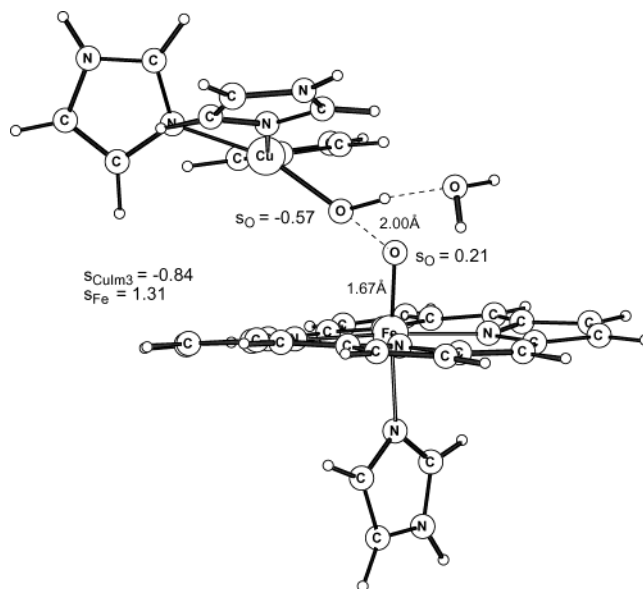


**Figure 16.** Approximate transition state for O–O bond cleavage obtained for a medium sized model including an extra proton.

will be presented in the opposite order, starting with the largest model as described in the previous sections, and then omitting piece by piece from that model, ending up with the initially used ones. The main conclusion as it turns out is that the results are quite stable with respect to the size of the model.

The comparison between different models will be concerned with the actual O–O bond cleavage step, i.e., the activation energy computed with respect to the peroxide intermediate labeled  $I_P$ . For the large model already discussed, the calculated barrier is 11.4 kcal/mol above  $I_P$ , determined as the maximum on the O–O bond stretching potential energy curve. A minor modification of the model is to remove the farnesyl hydroxyl group and its hydrogen bond to the tyrosyl hydroxyl group. When this structural strain is removed, it is enough to have only one water molecule bridging between the tyrosyl hydroxyl group and the oxygen molecule. For this model only the smaller basis set was used and no dielectric effects were calculated, but at that level, the O–O bond cleavage barrier relative to the preceding peroxide structure was found to be almost identical to the value obtained for the largest model at the same level, differing only by 0.2 kcal/mol.

At the stage of the O–O bond cleavage process discussed here, the tyrosyl residue is actually found not to be involved, and the next step of simplification of the model is therefore to omit the tyrosine. Also for this model the maximum on the O–O bond cleavage potential curve is found to occur close to 2.0 Å, and the structure is shown in Figure 16. In this model, one water molecule is introduced to simulate the hydrogen bonding link toward the tyrosyl hydroxyl group. For this model, using the large basis set but without dielectric effects (which for the largest model actually turned out to be zero for the barrier height relative to the  $I_P$  structure), a barrier of 13.9 kcal/mol was obtained, i.e., 2.5 kcal/mol higher than for the largest model. The spin populations at the transition state, as shown in Figure 16, agree reasonably

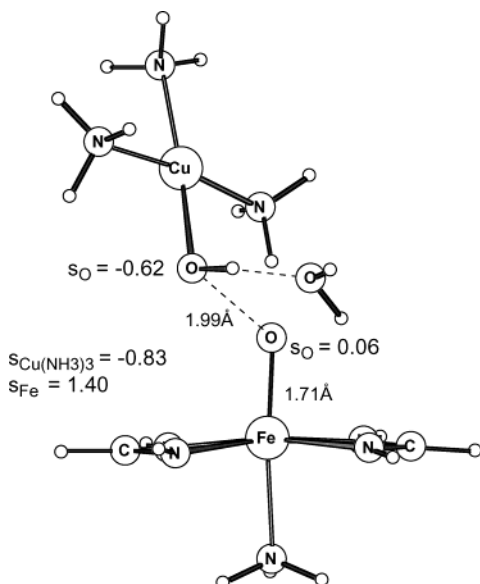


**Figure 17.** Fully optimized transition state for O–O bond cleavage obtained for a small model including an extra proton.

well with the results for the largest model, as shown in Figure 8. The main difference is that the spin populations being built up on the two oxygen atoms are somewhat smaller for the smaller model,  $-0.74$  and  $0.47$  for the large model, and  $-0.57$  and  $0.21$  for the smaller model.

The smallest model used is dramatically smaller, with the histidines modeled by ammonias (instead of imidazoles as used in the larger models) and the heme modeled by an iron ion with two chelating diformamidate ( $\text{NHCHNH}^-$ ) ligands (instead of an unsubstituted iron porphyrin as used in the larger models). One advantage with this small model is that a Hessian (i.e., the second derivatives of the energy with respect to the nuclear coordinates) could be calculated, and a true transition state optimization could be performed. The structure of the optimized transition state is shown in Figure 17, and at this point the Hessian has an imaginary frequency of  $127\text{ cm}^{-1}$  corresponding to stretching the O–O bond. The spin populations shown in Figure 17 for the smallest model agree reasonably well with those in Figure 8 for the largest model. The main difference in the spin populations is that for the small heme model the spin is shifted slightly from the oxo group toward iron. The barrier calculated for this small model is  $11.9\text{ kcal/mol}$ ,  $2\text{ kcal/mol}$  lower than for the model in Figure 16 which incorporates the same features as the smallest model. This barrier is very close to the  $11.4\text{ kcal/mol}$  obtained for the largest model in Figure 8. The small model is also used in an approximate determination of the barrier, constructing a one-dimensional potential energy surface for the O–O bond cleavage as was done for the large models. The latter procedure gives exactly the same result as for the true transition state optimization, indicating that the approximate procedure should be valid also for the larger models, where it is the only possibility.

The Hessians calculated for the smallest model can also be used to estimate zero point and thermal effects on the relative energies, applying the harmonic approximation. For the O–O bond cleavage barrier relative to the  $\text{I}_\text{P}$  peroxide

structure, these effects together decrease the barrier by  $1.2\text{ kcal/mol}$ , resulting in a free energy of activation of  $10.7\text{ kcal/mol}$  for the small model. If these effects are transferred to the largest model, the free energy of activation relative to the  $\text{I}_\text{P}$  structure for this model would be  $10.2\text{ kcal/mol}$ . The rate of  $\text{P}_\text{M}$  formation, however, is determined from the lifetime of compound A, since there is no stable structure observed corresponding to the  $\text{I}_\text{P}$  peroxide structure, and the experimental rate corresponds to a barrier of  $12.4\text{ kcal/mol}$  for the O–O bond cleavage reaction. As discussed, a value of  $5\text{ kcal/mol}$  is used for the free energy difference between compounds A and  $\text{I}_\text{P}$ , accounting for the fact that the peroxide is not observed. Using this estimate together with the calculated barrier for the largest model leads to a final estimate of the free energy of activation of  $15.2\text{ kcal/mol}$  for the O–O bond cleavage mechanism with an extra proton present in the binuclear center, very close to the experimental value of  $12.4\text{ kcal/mol}$ .

Another important experimental result is that the temperature dependence of the  $\text{O}_2$  activation reaction is found to be very weak, resulting in an estimated activation energy of only  $6.4\text{ kcal/mol}$  from an Arrhenius plot (the slope of  $\ln(k)$  versus  $1/T$ ).<sup>31</sup> This result indicates a large entropy effect, increasing the O–O bond cleavage barrier relative to compound A by as much as  $6\text{ kcal/mol}$ . Since compound A cannot be treated within the same model as used for the transition state determination, the entropy effect relative to compound A on the O–O bond cleavage reaction cannot be directly calculated. It can be noted that the entropy effect on the  $\text{I}_\text{P}$  to TS step, which is possible to compute, is very small, which means that the main entropy effect would have to occur between compound A and the  $\text{I}_\text{P}$  peroxide structure. The entropy effect for this step can be taken from a very similar reaction, starting from compound A in the same form as in Figure 15 and forming an Fe–OOH peroxide by splitting the copper coordinated water molecule. Such a reaction step was studied using the same type of small model as in Figure 17, and the entropy effect was found to be about  $7\text{ kcal/mol}$ , raising the peroxide structure. From these results, it is suggested that the mechanism with an extra proton proposed here actually is characterized by an entropy effect of about the same size as the one deduced from the experimental observations, i.e., raising the barrier by  $6\text{ kcal/mol}$ .

**IIIe. Summary: The Complete A to  $\text{P}_\text{M}$  Reaction.** In compound A, molecular oxygen is weakly bound to heme  $\text{a}_3$ , and in the next observed intermediate in the catalytic cycle of cytochrome oxidase, compound P, the dioxygen O–O bond is cleaved. This also occurs in the mixed valence form of the enzyme, where there is no electron available in the heme a cofactor, which could enter the binuclear center and assist the O–O bond cleavage process. In this case, the O–O bond cleaved intermediate is labeled  $\text{P}_\text{M}$ , and a possible mechanism for the O–O bond cleavage reaction in the mixed valence enzyme is presented here. According to the present calculations, the first step in cleaving the O–O bond is to

(31) Karpefors, M.; Ädelroth, P.; Namslauer, A.; Zhen, Y.; Brzezinski, P. *Biochemistry* **2000**, *39*, 14664.

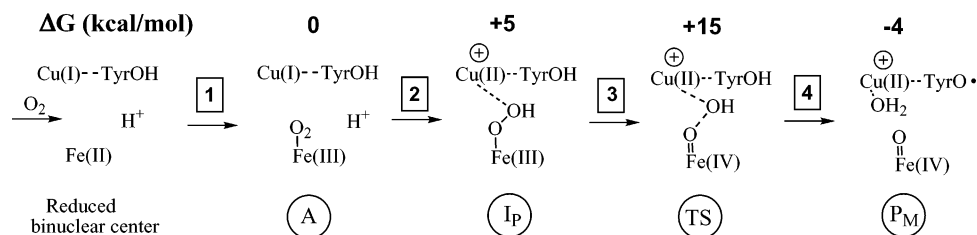


**Figure 18.** Mechanism suggested for the O–O bond cleavage in the mixed valence form of cytochrome oxidase. Each reaction step corresponds to the transfer of one electron to the O<sub>2</sub> molecule.

protonate the dioxygen. One possibility would be that the tyrosine hydroxyl group provides the proton, but the calculations show that such a process would lead to an O–O bond cleavage barrier that is too high by about 13 kcal/mol. On the other hand, the calculations also show that, with an extra proton available at the binuclear center, the O–O bond cleavage barrier decreases by 9 kcal/mol, leading to good agreement with the observed experimental lifetime for compound A. Experimental information shows that there is no proton taken up from the bulk during this step, and therefore, such a proton must be present in or near the binuclear center already in compound A.

The overall mechanism for the A to P<sub>M</sub> reaction emerging from the present calculations is summarized in Figure 18. To cleave molecular O<sub>2</sub> requires four electrons, which have to be transferred to the O<sub>2</sub> molecule from the binuclear center or its vicinity. Three of these electrons can be provided by the metal centers in the binuclear center, while the fourth electron has to be taken from somewhere else, which led to the suggestion of the formation of a tyrosyl radical. The process leading to the O–O bond cleaved P<sub>M</sub> product, and starting with the O<sub>2</sub> molecule coming into the reduced binuclear center, can then be divided into four steps, each one corresponding to the transfer of one of the four electrons, as depicted in Figure 18. The reduced form of the binuclear center has Fe(II) and Cu(I), and when the O<sub>2</sub> molecule is coordinated to iron, forming compound A, the first electron is transferred from iron to O<sub>2</sub>, leading to Fe(III). This is described as step 1 in Figure 18, but the energetics of this step are not discussed in the present paper, since the O–O bond cleavage barrier is determined with respect to compound A. In step 2, an electron is transferred from copper, leading to Cu(II) and a bridging peroxide labeled I<sub>P</sub> in the present paper. A main feature of the present mechanism is that in this step there is also a proton transfer to O<sub>2</sub>, and that, with the present number of electrons available at the binuclear center, this cannot be the tyrosine proton, but another proton available somewhere in the vicinity of the binuclear center. Since there is no peroxide intermediate observed experimentally, this step is estimated to be endergonic by 5 kcal/mol. In step 3, another electron is transferred from iron leading to Fe(IV) and a weakly bound intermediate with an elongated O–O bond. This step goes over a transition state which is calculated to be 10.2 kcal/mol above the I<sub>P</sub> structure, including zero point and thermal effects from a small model calculation, and thus about 15 kcal/mol above compound A. Finally, in step 4 an electron and a proton are taken from the tyrosine in the binuclear center leading to a

tyrosyl radical and the complete cleavage of the O–O bond. The energetics of this last step are difficult to calculate, since there are many different hydrogen bonding patterns possible here. However, it is clear that this step is exergonic and the value given in Figure 18 is taken from calculations on the separated metal complexes. Those calculations indicate that the I<sub>P</sub> to P<sub>M</sub> step is exergonic by 8.6 kcal/mol, which together with the A to I<sub>P</sub> endergonicity of 5 kcal/mol, leads to an exergonicity of 3.6 kcal/mol for the whole A to P<sub>M</sub> reaction. This mechanism thus leads to an estimated O–O bond cleavage barrier of about 15 kcal/mol, in good agreement with the value of 12.4 kcal/mol obtained from the lifetime of compound A in the mixed valence enzyme. Calculations on small model complexes furthermore indicate that there is a rather large entropy effect connected with step 2, which leads to a large entropy effect on the barrier, in good agreement with the observed low temperature dependence of the O–O bond cleavage reaction in the mixed valence enzyme.<sup>31</sup>

It is interesting to note that the present mechanism suggested for the mixed valence enzyme has some implications for the O–O bond cleavage reaction in the fully reduced enzyme. In this form of the enzyme, there is another electron available in one of the other cofactors, heme a, and this electron is transferred to the binuclear center during the O–O bond cleavage process leading to the O–O bond cleaved product labeled P<sub>R</sub>, having one more electron than P<sub>M</sub> at the binuclear center. The lifetime of compound A in the fully reduced enzyme is only slightly shorter than the one in the mixed valence enzyme, 50 μs as compared to 200 μs, corresponding to an O–O bond cleavage barrier very similar to the mixed valence enzyme, only 0.8 kcal/mol lower. This indicates that the O–O bond cleavage mechanism for the two forms of the enzyme should be similar. The present mechanism suggests that the fully reduced enzyme has the same mechanism as the mixed valence one up to step 4. In the fully reduced enzyme, the fourth electron could be taken directly from heme a, and no tyrosyl radical would then be formed.

Finally, it can only be speculated where in the binuclear center the extra proton, suggested by the calculations to be necessary for the O–O bond cleavage process, could be residing at the level of compound A. One possibility proposed in the previous computational paper<sup>16</sup> would be that the farnesyl hydroxyl group on heme a<sub>3</sub> is protonated as indicated in Figure 6. This hydroxyl group is located at the end of one of the proton channels, the K-channel, where at least one proton is transported to the binuclear center in

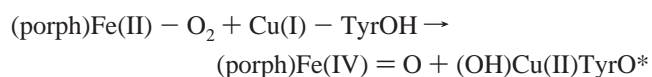
the reduction phase.<sup>32–34</sup> It was also argued in ref 16 that the proton affinity of this hydroxyl group should be unusually large due to its contact with the delocalized  $\pi$ -system of the porphyrin ring. However, it is not possible to obtain an accurate estimate of the proton affinity for that position within the present model. A slightly different possibility would be that the proton is located somewhat further away from the binuclear center, but still within the K-channel, stabilized by several groups in this part of the protein. A quite different possibility would be that the proton is supplied by the water molecule present in compound A near Cu<sub>B</sub> in the binuclear center.<sup>27</sup> In this case, the water molecule would have to be split into a proton, delivered to the oxygen dimer, and a hydroxyl group coordinating to copper. Preliminary calculations on such a mechanism indicate that, even if the first step of water cleavage seems to be energetically feasible, the later steps, leading up to the O–O bond cleavage, are very costly, resulting in a total barrier relative to compound A on the order of more than 30 kcal/mol. Other possibilities for the proton source could be the glutamic acid in the D-channel or one of the heme propionic groups. However, proton delivery from these sources would have to be coupled to rather complicated charge compensating movements, since electrometric measurements have shown that the reaction forming the P<sub>M</sub> state is not linked to net charge movement perpendicular to the membrane.<sup>35</sup>

#### IV. Conclusions

In this hybrid DFT (B3LYP) study, extensive models of the active site in cytochrome oxidase have been used to highlight the mechanism for the O–O bond cleavage process. The features of the active site included in the model are the porphyrin and axial histidine ligands of iron in heme a<sub>3</sub>, the three histidine ligands of Cu<sub>B</sub>, and the tyrosine cross-linked to one of these histidines. The purpose of the study was to elucidate the conditions for the O–O bond cleavage in the mixed valence form of the enzyme, i.e., under the assumption that there is no electron available to enter the active site from the outside during the bond cleavage process. The most accepted description of compound P<sub>M</sub>, the product of the O–O bond cleavage in the mixed valence enzyme, is that the metals are in the oxidation states Fe(IV) and Cu(II). This means that for the O–O bond cleavage to occur one electron has to be supplied by some residue in the surrounding protein, and the cross-linked tyrosine has been suggested as the source for this electron, forming a tyrosyl radical in P<sub>M</sub>. This is one reason for including the tyrosine residue in the calculations.

The simplest mechanism for the O–O bond cleavage fulfilling the experimental observations would be described

by the reaction



where also a proton is transferred from the tyrosine to form the copper ligated hydroxyl group in the product, see also the scheme in Figure 4. The calculations show that the thermodynamics for such a mechanism are feasible, but the barrier would be more than 10 kcal/mol too high to correspond to the experimental lifetime of compound A ((porph)Fe(II)–O<sub>2</sub>). The problem with this mechanism is that it is not possible to transfer both a proton and an electron at the same time from the tyrosine to the O<sub>2</sub> molecule during the O–O bond cleavage process. Thus, some modification of the conditions in the active site had to be introduced to obtain agreement with experiment. Since the assumption generally made is that there is no other electron available, the number of electrons could not be changed. On the other hand, it is not possible from experimental data to draw conclusions about the number of protons present at the active site for a particular intermediate, and it was therefore decided to investigate the effects of increasing the number of protons in compound A. Interestingly, the calculations show that if an extra proton is assumed to be present in the active site, the barrier is lowered by about 10 kcal/mol and good agreement with the experimental reaction rate is obtained. It was therefore concluded that an extra proton, apart from the tyrosyl proton, has to be available at the binuclear center for the O–O bond cleavage to occur with low enough barrier, yielding the reaction mechanism described in the schemes in Figures 6 and 18.

It should be stressed that these conclusions are drawn under the assumption that there is no other source for an extra electron available at the binuclear center. Thus, if the fourth electron in the mixed valence form of the enzyme has to be taken from tyrosine (or any other part included in the models discussed above), then another proton, apart from the tyrosine proton, has to be available at the binuclear center. Another scenario, not investigated here, would be that there is another residue in the vicinity of the binuclear center that could deliver an electron at an early stage of the O–O bond cleavage reaction. In that case, it may well be possible to cleave the O–O bond with a low barrier without an extra proton at the binuclear center. In such a case, the O–O bond cleavage process would initially end up with a tyrosinate and a radical on some other residue. After the O–O bond is cleaved, the radical might migrate to the tyrosine residue, giving a tyrosyl radical in compound P<sub>M</sub>. One possible candidate for such an electron donor could be the tryptophan (Trp236 of the bovine enzyme) that is  $\pi$ -stacking with one of the histidine ligands of copper. This tryptophan, which is as close to the metal centers as the tyrosine, is conserved in all heme–copper oxidases, and it is found to be essential

(32) Hosler, J. P.; Shapleigh, J. P.; Mitchell, D. M.; Kim, Y.; Pressler, M. A.; Georgiou, C.; Babcock, G. T.; Alben, J. O.; Ferguson-Miller, S.; Gennis, R. B. *Biochemistry* **1996**, *35*, 10776–10783.

(33) Jünemann, S.; Meunier, B.; Gennis, R. B.; Rich, P. *Biochemistry* **1997**, *36*, 14456–14464.

(34) Konstantinov, A. A.; Siletsky, S.; Mitchell, D.; Kaulen, A.; Gennis, R. B. *Proc. Natl. Acad. Sci. U.S.A.* **1997**, *94*, 9085–9090.

(35) Jasaitis, A.; Verkhovskaya, M.; Morgan, J. E.; Verkhovsky, M.; Wikström, M. *Biochemistry* **1999**, *38*, 2697–2706.

(36) Puustinen, A.; Wikström, M. Unpublished.

(37) Siegbahn, P. E. M. *Chem. Phys. Lett.* **2002**, *351*, 311–318.

(38) Baldwin, J.; Krebs, C.; Ley, B. A.; Edmondson, D. E.; Huynh, B. H.; Bollinger, J. M., Jr. *J. Am. Chem. Soc.* **2000**, *122*, 12195.

*O–O Bond Cleavage in Cytochrome c Oxidase*

for the functioning of the enzyme.<sup>36</sup> This kind of situation is actually found in ribonucleotide reductase (RNR), where a tryptophan radical is initially formed during the O–O bond

cleavage. A stable tyrosyl radical is formed only at a later stage in RNR.<sup>37,38</sup>  
IC034060S